Effect of Monomer Structure and Compressibility on the Properties of Multicomponent Polymer Blends and Solutions. 3. Application to PS(D)/PVME Blends

Jacek Dudowicz and Karl F. Freed*

The James Franck Institute and the Department of Chemistry, University of Chicago, Chicago, Illinois 60637

Received January 29, 1991; Revised Manuscript Received March 29, 1991

ABSTRACT: Comparisons between lattice cluster theory predictions and experiment for thermodynamic properties of compressible blends are presented for the specific case of PS(D)/PVME blends. These comparisons are also used as part of a more general study of the influence of monomer structure and compressibility on the properties of polymer blends. A series of 12 different vinyl monomer structures is used to examine how monomer structure affects the effective interaction parameter, χ_{eff}, from extrapolated zero-angle experimental neutron scattering and the heat and volume changes upon mixing. When the effective interaction parameter is evaluated in the incompressible limit for 66 model blends that differ only in the monomer structures, the slope of the composition dependence of χ_{eff} is found to range over several orders of magnitude. Using one adjustable parameter, the microscopic exchange energy, only four of the model blends are in rough accord with both the temperature and composition dependences of the PS/PVME neutron scattering data of Han et al. A consideration of the heat of mixing serves to differentiate strongly between these four cases and emphasizes the need for several different types of measurements on the same system if interest lies in obtaining meaningful microscopic information concerning structure and interactions in polymer blends. The nonzero experimental values for the volume change on mixing provide a stimulus for extending the lattice cluster theory to compressible blends where the three van der Waals energies serve as the only adjustable parameters. Certain blend properties are again shown to be very sensitive to the monomer structures. Residual discrepancies between lattice cluster theory predictions and experiments provide insights into theoretical and experimental studies to unravel further the influences of monomer structure and interactions on the bulk thermodynamic properties of compressible polymer blends.

I. Introduction

Earlier papers[1,2] in this series provide a systematic solution of the lattice model for compressible multicomponent polymer systems. Classic Flory–Huggins (FH) theory[3] emerges as the zeroth-order approximation, and corrections describe the influence of short-range correlations that are induced by packing and interactions. Of particular significance is the fact that the theory permits monomers to have internal structures and therefore to extend over several lattice sites. This has enabled us to study the detailed relationship between molecular monomer structure and the thermodynamic properties of melts, blends, and concentrated polymer solutions.

The lattice cluster theory (LCT)[1,2,4] evaluates corrections to the FH mean-field approximation in the form of a double expansion in $1/z$, where z is the lattice coordination number, and in the reduced nearest-neighbor van der Waals attractive interaction energies $\epsilon_{\alpha\beta}/k_BT$. Our previous paper[5] compares the LCT predictions with Monte Carlo simulations of the identical lattice model for concentrated polymer solutions. The good agreement obtained there has stimulated the extension of the theory in paper 1 to multicomponent compressible polymer systems[1] and the applications in paper 2 to binary polymer blends.[2] Paper 2 provides numerous illustrative computations of the influence of monomer molecular structure and compressibility on the effective interaction parameter χ_{eff}, as measured by small-angle neutron scattering, and on excess thermodynamic quantities. These studies focus on variations of χ_{eff}, ΔH^{mix}, and ΔV^{mix} with blend composition, temperature, pressure, molecular weights, and microscopic interaction energies $\epsilon_{\alpha\beta}$. While these computations demonstrate that monomer molecular structures have a considerable influence on χ_{eff}, ΔH^{mix}, and ΔV^{mix}, the range of this dependence has not been explored in systematic detail or for the extensive number of monomer structures considered here.

A theory for the thermodynamic properties of the polymer system must ultimately be formulated on the basis of detailed monomer molecular structure and information concerning specific interactions, but it is a priori unclear what details of structure and interactions are necessary to describe faithfully experiments. Thus, it is natural to study models that introduce sufficient elements of reality to elucidate the salient physical influences. The lattice model is, of course, an oversimplified representation of reality, but its mathematical simplicity permits a more complete solution of the model to be provided and tested against experimental data. After assuring that our approximation adequately represents the solution of the lattice model, deviations between theory and experiment indicate the limitations in the lattice model. The latter limitations may then be rectified by alterations of the model or, ultimately, by use of a nonlattice-based theory.

The present paper considers a wide range of vinyl monomer structures to determine how sensitive macroscopic thermodynamic quantities, such as χ_{eff}, ΔH^{mix}, and ΔV^{mix}, are to monomer molecular structure. Sensitivity of these properties to monomer structure implies the possibility of controlling blend properties through modification of monomer structure. On the other hand, this sensitivity means that experimental measurements of these quantities are truely probing microscopic interactions, local correlations, etc., in polymer systems. However, this interesting microscopic information may be extracted only by the use of theories that faithfully describe the dominant physical phenomena.

Section II summarizes the lattice model for structured monomers and the form of the LCT predictions for the free energy of a compressible binary blend. Definitions are provided of the small-angle scattering effective in-

0024-9297/91/2224-5112$02.50/0

teraction parameter χ_{eff} and of excess thermodynamic quantities. The Helmholtz free energy of papers 1 and 2 is converted to the Gibbs free energy, so that all computations may be performed at the constant pressure of 1 atm. (Pressure dependences are illustrated in paper 2.)

The discussion of general variations in the thermodynamic properties of binary incompressible blends in section III is followed by detailed comparisons of the LCT predictions with the extensive small-angle neutron scattering data of Han et al.[6] for PSD/PVME blends. These data are distinguished from those for other blends by being available as a function of both temperature and composition, thereby enabling us to perform several very stringent tests of LCT predictions. The comparisons of theory with experiment begin in section III by temporarily suspending knowledge of the actual monomer structures and by determining which of the 66 model binary incompressible blends can reproduce the neutron scattering data for χ_{eff} with but a single adjustable parameter, the microscopic exchange energy ϵ. These 66 model blends differ only in the structures assigned to the styrene and vinyl methyl ether monomers. Given fits to the extensive χ_{eff} data, no further adjustable parameters are available to our subsequent comparison of LCT predictions with experimental data of Shiomi et al.[7] for excess thermodynamic properties of PS/PVME blends.

Section IV continues the comparison with experiments for PS(D)/PVME systems by permitting the 66 model blends to be compressible. Compressibility implies that the LCT now has three adjustable parameters, the microscopic interaction energies ϵ_{S-S}, $\epsilon_{VME-VME}$, and ϵ_{S-VME}, in the simplest of possible models. The experimental comparisons indicate the relevance of compressibility for understanding χ_{eff}, ΔH^{mix}, and ΔV^{mix}, and they demonstrate some deficiencies in our extended lattice model with structured monomers. As explained in section V, several of these deficiencies may be remedied by available techniques, albeit at additional computational expense. Our goal here is not to provide a perfect fit to experiment but rather to examine the most relevant physical influences. The prediction of a strong dependence of certain blend thermodynamic properties on monomer molecular structure is probably the most important consequence of our analysis.

II. Model and Notation

The standard lattice model of a binary blend represents[3] the polymer chain conformations by placing identical segments (monomers) at the lattice sites of a regular array with coordination number z. The two chain species have $N^{(1)}$ and $N^{(2)}$ flexible backbone bonds joining these segments. Excluded-volume constraints apply to all monomers in the system and prohibit more than one of them to lie at the same lattice site. We consider hypercubic lattices, where the number of neighbors to a lattice site is $z = 2d$, with d the spatial dimensionality. The whole lattice has N_l total sites, and there are n_α chains of species $\alpha = 1$ or 2.

The standard lattice model[3] is quite deficient in taking each monomer to occupy only one lattice site, because, in reality, monomers of different species generally have varying sizes and shapes. However, our recent extension[1] of the lattice model more faithfully represents the molecular structure of compressible polymer blends by allowing monomers to cover several lattice sites according to their relative sizes and internal structures. For instance, some examples of vinyl monomer structures are given in Figure 1. Chains are formed from these structures by

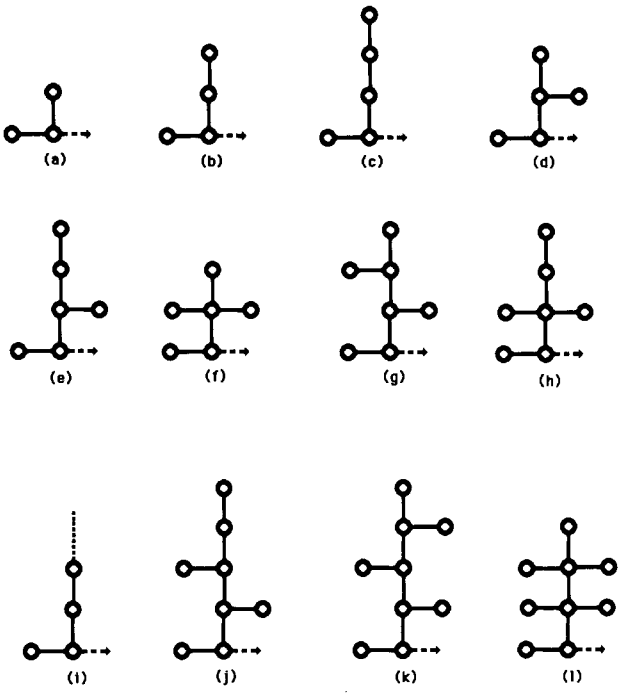

Figure 1. Examples of vinyl monomer structures that extend over s_α neighboring lattice sites. s_α varies from 3 for structure a to 9 for k and l. Polymer chains are constructed by linking monomers in the directions of the arrows to form vinyl polymer chains. All bonds are fully flexible in three dimensions.

linkages in the directions of the arrows. The monomers in structures a–l occupy s_a–s_l neighboring lattice sites, respectively, and all submonomer units are connected by flexible bonds. The chain site occupancy indices M_α, $\alpha = 1$, 2, are obtained by multiplying the number of monomers in a single chain by the number of lattice sites occupied by one monomer, $M_\alpha = (N^{(\alpha)} + 1)s_\alpha$. Composition may be represented, as convenient, in terms of volume fractions $\phi_\alpha = n_\alpha M_\alpha / N_l$, nominal volume fractions $\Phi_\alpha = n_\alpha M_\alpha / (n_1 M_1 + n_2 M_2)$ or experimental volume fractions $\phi_\alpha^{(exp)} = V_\alpha / (V_1 + V_2)$, defined in terms of the volumes V_α of pure components α.

The liquidlike excess free volume of a compressible system is modeled by the presence of n_ν unoccupied lattice sites with volume fraction $\phi_\nu = n_\nu / N_l = 1 - \phi_1 - \phi_2$. Compressibility also influences the treatment of interaction energies. While it is possible to permit different portions of each monomer to interact with different and specific energies, all portions of a monomer are taken here to interact with the same nearest-neighbor attractive van der Waals energies $\epsilon_{\alpha\beta}$, $\alpha, \beta = 1, 2$. Thus, a compressible blend has three independent energies ϵ_{11}, ϵ_{22}, and ϵ_{12}. Specific interactions for different portions of the same monomer can be easily introduced into the lattice cluster theory at the expensve only of greater algebraic complexity. Blend compressibility implies that a single exchange energy parameter $\epsilon \equiv \epsilon_{11} + \epsilon_{22} - 2\epsilon_{12}$ no longer describes excess thermodynamic quantities, which depend separately on the three different energies ϵ_{11}, ϵ_{22}, and ϵ_{12}.

Flory–Huggins (FH) theory[3] is originally formulated in terms of the standard lattice model, which ignores the correlations in subsegment positions necessary to distinguish between the properties of polymers containing the structured monomers of Figure 1. The lattice cluster theory[1,4,5] (LCT) provides systematic corrections to the FH mean-field approximation for the extended lattice model with structured monomers such as those in Figure 1. Our recent paper[2] (paper 2) presents the LCT noncombinatorial Helmholtz free energy, F, for a compressible

Table I
Combinatorial Factors $\{N_i\}$ for the Various Vinyl Chain Architectures Built from the Monomer Structures of Figure 1 (by Linking Monomers in the Directions of the Arrows and by Connecting Monomers by the Backbone Bonds)

structure	N_1	N_2	N_3	$N_\perp$	$N_{1,1}$	$N_{1,2}$
a	$\frac{3}{2}N^a$	$2N-1$	$2N-4$	$N/2$	$\frac{9}{8}N^2-\frac{11}{4}N+1$	$3N^2-11N+10$
b	$2N$	$\frac{5}{2}N-1$	$3N-4$	$N/2$	$2N^2-\frac{7}{2}N+1$	$5N^2-\frac{29}{2}N+10$
c	$\frac{5}{2}N$	$3N-1$	$\frac{7}{2}N-4$	$N/2$	$\frac{25}{8}N^2-\frac{17}{4}N+1$	$\frac{15}{2}N^2-17N+10$
d	$\frac{5}{2}N$	$\frac{7}{2}N-1$	$4N-4$	N	$\frac{25}{8}N^2-\frac{19}{4}N+1$	$\frac{35}{4}N^2-\frac{41}{2}N+10$
e	$3N$	$4N-1$	$5N-4$	N	$\frac{9}{2}N^2-\frac{11}{2}N+1$	$12N^2-24N+10$
f	$3N$	$5N-1$	$5N-4$	$\frac{5}{2}N$	$\frac{9}{2}N^2-\frac{13}{2}N+1$	$15N^2-\frac{61}{2}N+10$
g	$\frac{7}{2}N$	$5N-1$	$6N-4$	$\frac{3}{2}N$	$\frac{49}{8}N^2-\frac{27}{4}N+1$	$\frac{35}{2}N^2-30N+10$
h	$\frac{7}{2}N$	$\frac{11}{2}N-1$	$\frac{13}{2}N-4$	$\frac{5}{2}N$	$\frac{49}{8}N^2-\frac{29}{4}N+1$	$\frac{77}{4}N^2-35N+10$
i^b	$\frac{N}{2}(n+2)$	$\frac{N}{2}(n+3)-1$	$\frac{N}{2}(n+4)-4$	$N/2$	$\frac{N^2}{8}(n+2)^2-\frac{N}{4}(3n+8)+1$	$\frac{N^2}{4}(n+2)(n+3)-\frac{N}{2}(5n+19)+10$
j	$4N$	$\frac{11}{2}N-1$	$7N-4$	$\frac{3}{2}N$	$8N^2-\frac{15}{2}N+1$	$22N^2-\frac{67}{2}N+10$
k	$\frac{9}{2}N$	$\frac{13}{2}N-1$	$8N-4$	$2N$	$\frac{81}{8}N^2-\frac{35}{4}N+1$	$\frac{117}{4}N^2-\frac{79}{2}N+10$
l	$\frac{9}{2}N$	$8N-1$	$\frac{19}{2}N-4$	$\frac{9}{2}N$	$\frac{81}{8}N^2-\frac{41}{4}N+1$	$36N^2-53N+10$

[a] N is the number of bonds in the chain backbone. The site occupancy index M (the total number of sites occupied by a single chain) is equal to N_1-1 for all polymer structures. [b] n denotes the number of bonds in side groups of monomer i (see Figure 1). The $\{N_i\}$ are given here for $n \geq 2$.

binary blend with structured monomers in the simple analytic form of a polynomial in the volume fractions ϕ_α and ϕ_ν. Subtracting the contributions of pure components from F or, equivalently, neglecting terms linear in ϕ_α leads to the Helmholtz free energy of mixing, $\Delta F^{\rm mix}$, in the form

$$\frac{\Delta F^{\rm mix}}{N_l k_B T} = \phi_\nu \ln \phi_\nu + \frac{\phi_1}{M_1}\ln \phi_1 + \frac{\phi_2}{M_2}\ln \phi_2 + \frac{\Delta F^{\rm mix}_{\rm nc}}{N_l k_B T} \quad (2.1)$$

where the noncombinatorial portion $\Delta F^{\rm mix}_{\rm nc}$ can be written in compact notation as

$$\frac{\Delta F^{\rm mix}_{\rm nc}}{N_l k_B T} = g_{12}\phi_1\phi_2 + g_{1\nu}\phi_1\phi_\nu + g_{2\nu}\phi_2\phi_\nu \quad (2.2)$$

The coefficients $g_{12}(\phi_1,\phi_\nu)$, $g_{1\nu}(\phi_1,\phi_\nu)$, and $g_{2\nu}(\phi_2,\phi_\nu)$ are functions of composition. Individual coefficients of powers of ϕ_1, ϕ_2, and ϕ_ν in these $g_{\alpha\beta}$ are expanded in the inverse coordination number $1/z$ and the three microscopic interaction energies ϵ_{11}, ϵ_{22}, and ϵ_{12} in units of the thermal energy k_BT. The coefficients in this double series are written in terms of site occupancy indices M_α and a set of geometrical factors $N_i^{(\alpha)}$, $N_{i,j}^{(\alpha)}$, $N_\perp^{(\alpha)}$, etc., that depend on monomer molecular structures as follows: $N_i^{(\alpha)}$ is the number of distinct ways of selecting sequential sets of i bonds in one polymer of species α that covers M_α sites; $N_{i,j}^{(\alpha)}$ is the number of ways of selecting nonsequential sets of i sequential and j sequential bonds in a single chain α, whereas $N_\perp^{(\alpha)}$ is the number of ways in which three bonds of one chain α meet at a single lattice site. Table I presents those counting indices for homopolymers composed of the vinyl monomer structures a–l of Figure 1 that are required in eq 2.2 for $\Delta F^{\rm mix}_{\rm nc}$. The single analytic expression (2.2) applies to binary blends of all compositions, molecular weights, temperatures, flexible monomer molecular structures, and van der Waals interactions $\epsilon_{\alpha\beta}$. It is this enormous generality of the LCT and the relative analytical simplicity of the results that enable us to consider the wide range of computations that would otherwise become prohibitive with numerical solutions of realistic off-lattice models.

The quantities $g_{\alpha\nu}\phi_\alpha\phi_\nu$ in (2.2) represent the reduced noncombinatorial free energies for mixing of pure polymers and voids, i.e., the free energies of the compressible melts. The separation of an "interaction" portion in $\Delta F^{\rm mix}_{\rm nc}$ [the g_{12} term in (2.2)] from that for pure melts (the $g_{1\nu}$ and $g_{2\nu}$ terms) is made only for comparison with phenomenological pairwise additive models. The g_{12} from Table I in paper 2 exhibits a dependence of g_{12} on ϕ_ν that violates the additivity assumptions in prior phenomenological models. The $g_{\alpha\beta}$ ($\alpha = 1, 2$, $\beta = 2, \nu$, and $\beta \neq \alpha$) in (2.2) are expanded in a double series in z^{-1} and $\epsilon_{\alpha\beta}$ through order z^{-2} and $\epsilon_{\alpha\beta}^2$ in the form

$$g_{\alpha\beta} = \sum_{m_\alpha,m_\nu=0} \phi_\alpha^{\,m_\alpha}\phi_\nu^{\,m_\nu} C_{m_\alpha,m_\nu} \quad (2.3)$$

with the LCT expansion having the structure $C_{m_\alpha,m_\nu} = \sum_{p,q}(z)^{-p}(\epsilon_{\alpha\beta})^q C^{(pq)}_{m_\alpha,m_\nu}$, where terms in $(\epsilon_{\alpha\beta})^2$ schematically represent quadratic contributions like $\epsilon_{11}\epsilon_{12}$, $\epsilon_{11}\epsilon_{22}$, ϵ_{11}^2, etc., and $\epsilon_{\alpha\nu} \equiv \epsilon_{\alpha\alpha}$. Table I of paper 2 contains terms through order z^{-2} in $\epsilon_{\alpha\beta}^0$, through order z^{-1} in $\epsilon_{\alpha\beta}$, and through order z^0 in $(\epsilon_{\alpha\beta})^2$. The results are in good agreement with Monte Carlo simulations[5] for the incompressible polymer–solvent (or, equivalently, the compressible polymer-void) system.

Because most experiments are performed at fixed pressure P, it is convenient to convert the Helmholtz free energy of mixing the Gibbs free energy of mixing

$$\Delta G^{\rm mix} \equiv \Delta F^{\rm mix} + P\Delta V^{\rm mix} \quad (2.4)$$

by specifying the pressure P and by computing the volume of mixing $\Delta V^{\rm mix}$ from the equation of state. The pressure P is evaluated from the Helmholtz free energy F as

$$P \equiv -\left.\frac{\partial F}{\partial V}\right|_{T,n_1,n_2} = -\left.\frac{1}{a^3}\frac{\partial F}{\partial n_\nu}\right|_{T,n_1,n_2} = -\left.\frac{1}{a^3}\frac{\partial \Delta F^{\rm mix}}{\partial n_\nu}\right|_{T,n_1,n_2} \quad (2.5)$$

where the derivative with respect to n_ν is expressed more

conveniently as

$$\left.\frac{\partial \Delta F^{mix}}{\partial n_\nu}\right|_{T,n_1,n_2} = -\frac{\phi_1}{N_l}\left.\frac{\partial \Delta F^{mix}}{\partial \phi_1}\right|_{T,\phi_2,\phi_\nu} - \frac{\phi_2}{N_l}\left.\frac{\partial \Delta F^{mix}}{\partial \phi_2}\right|_{T,\phi_1,\phi_\nu} + \frac{(1-\phi_\nu)}{N_l}\left.\frac{\partial \Delta F^{mix}}{\partial \phi_\nu}\right|_{T,\phi_1,\phi_2} \quad (2.5a)$$

and where a denotes the lattice constant. The equation of state is obtained analytically from (2.5), (2.2), and (2.1), and it enables the numerical determination of ϕ_ν as a function of P and other state variables (M_1, M_2, Φ_1, T, a). An analogous procedure is applied to the equations of state for the pure melts to yield the void volume fractions $\phi_\nu^{(\alpha)}$ in the compressible melt of pure component α. The relative volume change on mixing $\Delta V^{mix}/(V_1 + V_2)$ is then determined from

$$\frac{\Delta V^{mix}}{V_1+V_2} \equiv \frac{V - V_1 - V_2}{V_1+V_2} = \frac{1}{\Phi_1^* + \Phi_2^*} - \frac{1}{1+\Phi_1^*/\Phi_2^*} - \frac{1}{1+\Phi_2^*/\Phi_1^*} \quad (2.6)$$

where the notation $\Phi_\alpha^* \equiv \phi_\alpha/(1-\phi_\nu^{(\alpha)})$ is introduced.

As described in ref 2, knowledge of the Gibbs free energy, G, for a binary blend enables the calculation of the extrapolated zero-angle coherent neutron scattering partial structure factor, $S_{11}(0)$, and the corresponding site–site Flory effective interaction parameter, χ_{eff}, which *is defined by*

$$\chi_{eff} = -\frac{1}{2}\left[S_{11}(0)^{-1} - \frac{1}{M_1\phi_1^{(exp)}} - \frac{1}{M_2\phi_2^{(exp)}}\right] \quad (2.7)$$

Neutron scattering experimentalists sometimes analyze[6] their data in terms of a site volume effective interaction parameter χ'_{eff}, which is defined by

$$\frac{\chi'_{eff}}{\nu_o} = -\frac{1}{2}\left[\frac{S_{11}(0)^{-1}}{\nu_c} - \frac{1}{(N^{(1)}+1)\nu_1\phi_1^{(exp)}} - \frac{1}{(N^{(2)}+1)\nu_2\phi_2^{(exp)}}\right] \quad (2.8)$$

and differs from (2.7) by the appearance of the reference unit cell volume $\nu_o = (\nu_1\nu_2)^{1/2}$, the volumes ν_α, $\alpha = 1, 2$, of a single monomer, the polymerization indices $N^{(\alpha)}$, and the cell volume ν_c. (Equations 2.7 and 2.8 apply to the simple limit of complete contrast, but the incomplete case is readily treated.) The two χ_{eff} in (2.7) and (2.8) are related to each other by

$$\chi'_{eff} = (s_1 s_2)^{1/2}\chi_{eff} \quad (2.8a)$$

where the conversion factor $(s_1s_2)^{1/2}$ explicitly depends on the monomer structures of the two blend components.

Other thermodynamic quantities are simply evaluated from standard thermodynamic formulas. For example, the internal energy of mixing is computed as

$$\Delta E^{mix} = \partial[\Delta F^{mix}/k_BT]/\partial[(k_BT)^{-1}] \quad (2.9)$$

and the heat of mixing is obtained from

$$\Delta H^{mix} = \partial[\Delta G^{mix}/k_BT]/\partial[(k_BT)^{-1}] \quad (2.9a)$$

These two quantities are considered in the following sections for compressible blends of structured monomers. Since meaningful calculations of these thermodynamic properties are defined for a stable homogeneous one-phase blend, it is necessary to check the blend stability for each set of M_1, M_2, Φ_1, P, T, and a. The conditions for stability of a binary polymer blend at constant pressure P and temperature T are

$$\left.\frac{\partial^2 G}{\partial \Phi_1^{\,2}}\right|_{P,T} > 0 \quad (2.10)$$

All calculations presented below are carried out for a pressure of P = 1 atm, the coordination number z = 6, and the molal reference unit cell volume $N_A\nu_o$ = 74.66 cm^3/mol that is obtained from Han.[8] (N_A is Avogadro's number.) The lattice constant a is then naturally defined by $a = [\nu_o/(s_1s_2)^{1/2}]^{1/3}$.

III. Flory Effective Parameter χ_{eff}^{inc} and the Internal Energy of Mixing ΔE_{inc}^{mix} for Incompressible Limit Binary Blends: Dependence on Monomer Molecular Structure

The incompressible limit is considered first because incompressible models are generally used to analyze small-angle neutron scattering data. The influence of compressibility is studied in section IV. An incompressible binary blend lacks excess free volume (ϕ_ν = 0) and, consequently, exhibits no pressure. The incompressible blend neutron scattering intensity and excess thermodynamic quantities then depend, for a given set of M_1, M_2, T, z, and monomer structures, only on a single exchange energy parameter $\epsilon \equiv \epsilon_{11} + \epsilon_{22} - 2\epsilon_{12}$. This section illustrates some general variations of the effective interaction parameter, χ_{eff}^{inc}, and the internal energy of mixing, ΔE_{inc}^{mix} with molecular monomer structure when all molecular parameters other than ϵ are fixed but when only the monomer structures are permitted to vary. The value of ϵ is chosen to provide a fixed value of $S_{11}(0)$ at a particular composition as described below.

The incompressible blend effective interaction parameter, χ_{eff}^{inc}, simply follows from the noncombinatorial Helmholtz free energy of mixing, $\Delta F'^{mix}_{nc}$ [obtained from (2.2) by setting ϕ_ν = 0] as

$$\chi_{eff}^{inc} = -\frac{1}{2}\left.\frac{\partial^2[\Delta F'^{mix}_{nc}/(N_l k_B T)]}{\partial \phi_1^{\,2}}\right|_{T,N_l} = \chi_S^{inc} + \chi_E^{inc} \quad (3.1)$$

where the prime on ΔF designates an incompressible blend (ϕ_ν = 0) and where both entropic χ_S^{inc} and energetic χ_E^{inc} portions of χ_{eff}^{inc} are polynomials in the volume fraction $\phi_1 = 1 - \phi_2$. The LCT series expansions of the macroscopic interaction parameter are written as

$$\chi_S^{inc} = \chi_S^{(0)} + \chi_S^{(1)}\phi_1 + \chi_S^{(2)}\phi_1^{\,2} + \dots \quad (3.2)$$

$$\chi_E^{inc} = [\chi_{E_1}^{(0)} + \chi_{E_1}^{(1)}\phi_1 + \chi_{E_1}^{(2)}\phi_1^{\,2} + \dots](\epsilon/k_BT) + [\chi_{E_2}^{(0)} + \chi_{E_2}^{(1)}\phi_1 + \chi_{E_2}^{(2)}\phi_2 + \dots](\epsilon/k_BT)^2 + \dots \quad (3.3)$$

The coefficients $\chi_S^{(j)}$, $\chi_{E_1}^{(j)}$, and $\chi_{E_2}^{(j)}$ in (3.2) and (3.3) depend on molecular structure and are given in Table II through orders z^{-2} and ϵ^2 in terms of site occupancy indices M_1 and M_2 and geometrical factors $N_i^{(\alpha)}$, $N_{i,j}^{(\alpha)}$, and $N_\perp^{(\alpha)}$. The definition (3.1) is equivalent to the expression (2.6) since an incompressible binary blend has $\phi_\alpha^{(exp)}$ simply equal to ϕ_α. Therefore, the zero-angle scattering becomes $S_{11}^{inc}(0)^{-1} = \partial^2[\Delta F'^{mix}/(N_l k_B T)]/\partial\phi_1^2$.

In the long-chain limit of M_1 and $M_2 \to \infty$, the entropic interaction parameter χ_S^{inc} is determined only by $N_2^{(1)}$ and

$N_2^{(2)}$ as

$$\chi_S^{inc} \rightarrow \chi_S^{(0)} = \frac{1}{z^2}\left[\frac{N_2^{(1)}}{M_1} - \frac{N_2^{(2)}}{M_2}\right]^2 \tag{3.4}$$

Thus, χ_S^{inc} vanishes for blends where both components have monomers with identical structures and otherwise is always nonnegative. The long-chain limit χ_S^{inc} is taken to provide a measure of the asymmetry of the two components, with the special case of $\chi_S^{inc} = 0$ corresponding to a symmetrical binary polymer blend.

Neglecting the ϵ^2 terms in (3.3) for now (this is permissible for small ϵ because the coefficients $\chi_{E_1}^{(0)}$ and $\chi_{E_2}^{(0)}$ in (3.3) are of order unity) and substituting χ_S^{inc} and χ_E from Table II and (3.2) and (3.3) into the right-most side of (3.1) leads to the long-chain limit of χ_{eff}^{inc} being linearly dependent on composition ϕ_1 with the general form

$$\chi_{eff}^{inc} = \chi_S^{(0)} + (\epsilon/k_BT)\chi_{E_1}^{(0)} + [(\epsilon/k_BT)\chi_{E_1}^{(1)} + \chi_S^{(1)}]\phi_1 \tag{3.5}$$

$$\equiv \chi_{eff}^{(0)} + \chi_{eff}^{(1)}\phi_1 \tag{3.5a}$$

The coefficients $\chi_S^{(0)}$, $\chi_S^{(1)}$, $\chi_{E_1}^{(0)}$, and $\chi_{E_1}^{(1)}$ depend explicitly on the monomer structures of the two blend components.

A. General Variation of Blend Properties with Monomer Structures. Any of the 12 vinyl monomer structures of Figure 1 may be chosen for each blend component, giving 132 possible model binary blends of components with different monomer structures. The component with the larger monomer (i.e., larger s_α) is taken as component 1 (without loss of generality), while when both species have monomers with the same s_α, component 1 is ascribed to polymer chains with a higher "branching ratio" $r_{br}^{(\alpha)} \equiv N_2^{(\alpha)}/M_\alpha$. This reduces the possibilities to 66 model blends.

Although our intention in this subsection is to consider general variations with monomer structure, it is convenient for subsequent sections to specify values of M_1, M_2, and T that are appropriate to the SANS experiments of Han et al.[6] for PSD/PVME blends. The chain site occupancy indices are chosen as $M_1 = s_1 M_w^{(PSD)}/M_{mon}^{(SD)}$ and $M_2 = s_2 M_w^{(PVME)}/M_{mon}^{(VME)}$, where s_α is the number of lattice sites occupied by one monomer of chain α and $M_{mon}^{(\alpha)}$ and $M_w^{(\alpha)}$ are molecular weights for a single monomer and for a single chain of polymer species α, respectively. The specific values $M_w^{(PSD)} = 593 \times 10^3$ and $M_w^{(PVME)} = 1100 \times 10^3$ and temperature $T = 142$ °C correspond to the small-angle neutron scattering (SANS) experiments for the PSD/PVME blends. We now use the above three parameters to consider the general case of the 66 model binary blends.

The only remaining parameter in the incompressible blend theory is ϵ. The exchange energy ϵ may be determined by using the theory of Table II from a single input value for $\chi_{eff}(\phi_1)$ or equivalently for $S_{11}(0)$ at a given ϕ_1. All 66 examples are placed on a common footing by choosing a fixed value of $S_{11}(0)$ such that $\chi_{eff}(\phi_1=0) \equiv 0$, a choice that simplifies some of the analysis. However, the results may be converted to other input values of $\chi_{eff}(\phi_1)$ as described below. The reference value $\chi_{eff}(\phi_1=0) = 0$ actually turns out to be close to the (extrapolated $\phi_1^{(exp)} \rightarrow 0$ limit) experimental data of Han et al.[6] for $T = 142$ °C, but it suffices as a reference value for the purposes of studying the general variation of blend properties with monomer molecular structures.

Given the large M_α values chosen, the computed $\chi_S^{(1)}$ is very small for the 66 model blends, so it is neglected in the equations of this subsection (but not in the final

Table II
Effective Interaction Parameter χ_{eff} to the Order of ϵ^2 for a Binary Incompressible Blend ($\phi_1 + \phi_2 = 1$)

$$\chi_{eff} = [\chi_S^{(0)} + \epsilon\chi_{E_1}^{(0)} + \epsilon^2\chi_{E_2}^{(0)}] + \phi_1[\chi_S^{(1)} + \epsilon\chi_{E_1}^{(1)} + \epsilon^2\chi_{E_2}^{(1)}] + \phi_1^2[\chi_S^{(2)} + \epsilon\chi_{E_1}^{(2)} + \epsilon^2\chi_{E_2}^{(2)}] + \phi_1^3[\epsilon\chi_{E_1}^{(3)} + \epsilon^2\chi_{E_2}^{(3)}] + \phi_1^4\epsilon^2\chi_{E_2}^{(4)}$$

$$\chi_S^{(0)} = \frac{1}{z}\Delta_1^2 + \frac{1}{z^2}\sum_{i=1}^{3} A_i$$

$$A_1 = -2\Delta_1(2\Delta_2 + \Delta_3 + 3\Delta_\perp + \Delta_{1,2} - 2\Delta_1\Delta_{1,1}) + \Delta_2^2$$
$$A_2 = 4N(1,2)\,[2 + 3N(1,2)]\Delta_1^2$$
$$A_3 = 4\Delta_1[[N(1,1) + N(1,2)]\,K(1,1;1) - 2N(1,2)\,K(1,1;2)]$$

$$\chi_{E_1}^{(0)} = \frac{z}{2} - 2\delta_1 + \frac{2}{z}\sum_{i=1}^{3} B_i$$

$$B_1 = -N(1,1)\,N(1,2) - 4N(2,1)\,N(1,2) + 2N(2,2)\,N(1,1)$$
$$B_2 = 2\delta_2 + \delta_3 + 3\delta_\perp + \delta_{1,2} - 4N(1,2)\,\delta_{1,1}$$
$$B_3 = 2K(1,1;1)\,\Delta_1 + 2[1 + N(1,2)]\Delta_1^2$$

$$\chi_{E_2}^{(0)} = \frac{z}{4} - 3N(1,1) + \frac{1}{2}N(1,2) - 3N(2,1) + [N(1,1)]^2 - 4K(1,1;1)$$

$$\chi_S^{(1)} = \frac{4}{z^2}[2\Delta_1 + 6N(1,2)\Delta_1 + 3\Delta_{1,1}]\Delta_1^2$$

$$\chi_{E_1}^{(1)} = 3\Delta_1 - \frac{3}{z}\sum_{i=1}^{3} C_i$$

$$C_1 = 2\Delta_2 + \Delta_3 + 3\Delta_\perp + \Delta_{1,2} + 8\Delta_1\delta_{1,1} - 4N(1,2)\Delta_{1,1}$$
$$C_2 = -4N(1,2)\,N(2,1) + 4N(1,1)\,N(2,2)$$
$$C_3 = 4\,[2 + 3\,N(1,2) - N(1,1)]\Delta_1^2$$

$$\chi_{E_2}^{(1)} = -\frac{3}{2}z + 3\sum_{i=1}^{2} D_i$$

$$D_1 = \frac{13}{2}N(1,1) - \frac{5}{2}N(1,2) + 3N(2,1) + N(2,2)$$
$$D_2 = -3[N(1,1)]^2 + [N(1,2)]^2 + 6K(1,1;1) - 3\Delta_1^2$$

$$\chi_S^{(2)} = \frac{12}{z^2}\Delta_1^4$$

$$\chi_{E_1}^{(2)} = \frac{24}{z}[\Delta_{1,1} + [1 + 3N(1,2) - 2N(1,1)]\Delta_1]\Delta_1$$

$$\chi_{E_2}^{(2)} = \frac{3}{2}z + 6\sum_{i=1}^{2} F_i$$

$$F_1 = -6N(1,1) + 4N(1,2) - N(2,1) - N(2,2)$$
$$F_2 = 3[N(1,1)]^2 - 2[N(1,2)]^2 - 4K(1,1;1) + K(1,1;2) + 9\Delta_1^2$$

$$\chi_{E_1}^{(3)} = \frac{40}{z}\Delta_1^3$$

$$\chi_{E_2}^{(3)} = 10[2\Delta_1 - \Delta_{1,1} - [N(1,1)]^2 + [N(1,2)]^2 - 9\Delta_1^2]$$

$$\chi_{E_2}^{(4)} = 45\Delta_1^2$$

where
$N(i,l) \equiv N_i^{(l)}/M_l$, $l = 1, 2$
$N(i,j;l) \equiv N_{i,j}^{(l)}/M_l$, $l = 1, 2$
$K(i,j;l) \equiv N(i,j;l) - \left(\frac{1}{2}\right)^{\delta(i,j)} N(i,l)N(j,l)M_l$, $l = 1,2$
$\Delta_i \equiv N(i,1) - N(i,2)$
$\delta_i \equiv N(i,1) - \frac{1}{2}N(i,2)$
$\Delta_{i,j} \equiv K(i,j;1) - K(i,j;2)$
$\delta_{i,j} \equiv K(i,j;1) - \frac{1}{2}K(i,j;2)$
$\delta(i,j) = 1$, $i=j$
$= 0$, otherwise

Table III
Entropic Interaction Parameter $\chi_S \times 10^5$ in the Upper Triangle as a Function of Monomer Structure with the Columns Labeling the PS Monomer Structure and the Rows Labeling the PVME Monomer Structure and the Lower Triangle Presenting the Slope $\chi_{eff}^{(1)} \times 10^5$ with Rows now Labeling the PS Monomer Structure and the Columns Labeling the PVME Monomer Structure

	a	b	c	d	e	f	g	h	i	j	k	l
a		19.2	49.4	12.3	−0.03	309	25.2	157	121	4.81	34.3	549
b	−0.93		7.03	62.5	19.3	482	88.6	287	43.4	43.4	105	774
c	6.74	1.24		111	49.3	605	145	383	15.6	85	166	927
d	−0.97	−1.82	−27.7		2.3	198	2.26	81.6	210	1.72	5.48	396
e	0.003	−0.95	−13.5	−0.24		309	25.3	158	121	4.87	34.3	54.9
f	−30.8	−23.7	−166	−3.83	60.4		157	25.2	81.5	236	137	34.3
g	−2.9	−5.65	−42.4	−0.08	4.35	−2.19		56.7	256	7.96	0.7	339
h	−25.7	−31.4	−134	−6.36	21.5	−1.44	−2.43		554	107	44.8	118
i	2.78	2.96	−2.04	19.9	32	91.2	31.8	88.8		174	283	1184
j	−0.61	−3.25	−26	−0.08	0.74	−5.8	−0.08	33.3	−26.7		134	451
k	−4.67	−8.8	−52.6	−0.29	4.53	−4.52	−0.01	1.04	−46.3	−0.11		309
l	−140	−153	−425	−64.8	22.4	−4.84	−42.5	−9.35	−339	−51.2	−32.3	

Table IV
Upper Triangle Gives $(\epsilon/kT) \times 10^5$ as a Function of Monomer Structure with Columns Labeling the PS Monomer Structure and the Rows Labeling the PVME Monomer Structure and the Lower Triangle Gives ΔE^{mix} (J/g) $\times 10^3$ for $\phi_1 = \phi_2 = 1/2$ and a Temperature of 142 °C, with Rows Labeling the PS Monomer Structure and Columns Labeling the PVME Monomer Structure

	a	b	c	d	e	f	g	h	i	j	k	l
a		−11.2	−25.3	−7.3	0.015	−185	−15.3	−98.2	−66.8	−2.94	−21	−361
b	−7.51		−3.54	−36.4	−11.4	−285	−52.8	−176	−23.7	−26	−63.4	−500
c	−19.6	−3.15		−69.4	−31.2	−383	−92.9	−253	−9.08	−54.8	−108	−649
d	−5.46	−31.2	−68.8		−7.2	−115	−1.33	−49.5	−114	−1.02	−3.27	−254
e	0.01	−10.7	−33.8	−7.5		−168	−13.9	−89	−61.4	−2.7	−19.3	−328
f	−152	−267	−416	−120	−184		−92.3	−15.2	−438	−139	−81.4	−21.8
g	−13.4	−53.3	−108	−1.5	−16.5	−113		−34	−137	−4.67	−0.41	−214
h	−86	−177	−294	−55.3	−105	−18.5	−44.6		−292	−62.1	−26.1	−73.7
i	−64.3	−26.1	−11.6	−139	−79.8	−589	−198	−421		−107	−175	−787
j	−2.76	−28	−68.3	−1.23	−3.44	−183	−6.59	−87	−165		−7.89	−284
k	−21	−72.3	−142	−4.15	−26	−113	−0.62	−38.7	−287	−12.6		−194
l	−355	−564	−847	−318	−436	−29.7	−315	−108	−1274	−446	−322	

numerical calculations). The parameter ϵ may be determinated by substituting $\chi_{eff}^{inc} = 0$ and $\phi_1 = 0$ into (3.5) along with $\chi_S^{(0)}$, $\chi_{E_1}^{(0)}$, and $\chi_{E_1}^{(1)}$ as calculated from Table II. This procedure gives

$$(\epsilon/k_B T) = -\chi_S^{(0)}/\chi_{E_1}^{(0)} \tag{3.6}$$

The slope of the linear composition dependence of χ_{eff}^{inc} on ϕ_1 in (3.5a) is then evaluated as $\chi_{eff}^{(1)} \equiv (\epsilon/k_B T)\chi_{E_1}^{(1)} + \chi_S^{(1)}$.

The computed $\chi_S^{(0)}$ and $\chi_{eff}^{(1)}$ are presented for the 66 model binary blends at $T = 142$ °C in Table III. The table is in the form of a matrix, where the matrix indices are a pair of vinyl monomer structures from Figure 1. The elements of the upper triangle of the matrix are the $\chi_S^{(0)}$, with the column index labeling the monomer structure of component 1 (later to be associated with PSD), while the row index designates the monomer architecture of component 2 (to be associated with PVME in subsection B below). The lower triangle displays the computed slopes $\chi_{eff}^{(1)}$ and is constructed in the reverse manner: the column indices refer to the monomer structure for species 1 and the rows to component 2. Table III, thus, illustrates the general variations of the incompressible LCT $\chi_S^{(0)}$ and $\chi_{eff}^{(1)}$ with molecular monomer structures. It simultaneously enables consideration of which of the 66 incompressible structured monomer binary model blends best reproduces the PS(D)/PVME experimental data of Han et al. for χ'_{eff}/v_o, a question that is addressed in more detail in subsection B and section IV. Other input values for $\chi_{eff}^{inc}(\phi_1)$ are also treated below.

The composition-independent entropic contribution $\chi_S^{(0)}$ to χ_{eff}^{inc} is always nonnegative in the long-chain limit of M_1 and $M_2 \to \infty$ (see eq 3.4). However, because finite M_1 and M_2 are used, it is possible to obtain very small negative $\chi_S^{(0)}$. An example is the $\chi_S^{(0)} = -0.03 \times 10^{-5}$ in the upper triangle of Table III for the $a-e$ incompressible blend. This special case has $(N_2^{(a)}/M_a - N_2^{(e)}/M_e)^2$ vanish, so $\chi_S^{(0)}$ would likewise vanish in the infinite M_α limit. Finite molecular weights, however, tend to make $\chi_S^{(0)}$ more negative (see paper 2). The $\chi_S^{(0)}$ values in Table III vary over 3 orders of magnitude for the 66 model binary incompressible blends and become as large as 10^{-2} for the most asymmetrical blends.

As we range over the 66 different monomer structure pairs, the slope $\chi_{eff}^{(1)}$ may have either sign. The values presented in the lower triangle matrix of Table III lie between −0.004 25 and +0.000 88 and vary over 5 orders of magnitude for a given sign. The computed dimensionless exchange energy parameter $(\epsilon/k_B T)$ also depends on monomer structure. Table IV is constructed in the same fashion as Table III and summarizes (in the upper triangle) the computed values of $(\epsilon/k_B T)$ for the 66 model blends. The lower matrix triangle in Table IV provides the internal energy of mixing ΔE_{inc}^{mix} (in J/g) calculated for a symmetrical composition $\phi_1 = \phi_2 = 0.5$ and $T = 142$ °C. ΔE_{inc}^{mix} is evaluated from the incompressible analogue of eq 2.9 and is likewise very sensitive to monomer structures as exhibited by Table IV.

The strong dependence of ϵ, ΔE_{inc}^{mix}, and the slope of χ_{eff}^{inc} vs ϕ_1 for a given choice of M_α, T, and $\chi_{eff}^{inc}(\phi_1 = 0)$ on monomer structures is probably the most interesting and significant feature of the lattice cluster theory for structured monomer polymers. The same sensitivity to monomer structure is obtained if the calculations are redone using the same value of ϵ for all 66 model blends rather than the same reference $\chi_{eff}^{inc}(\phi_1 = 0)$. The calculated slope

$\chi_{eff}^{(1)}$ then also varies with monomer structures by over 2 orders of magnitude (for both positive and negative $\chi_{eff}^{(1)}$). The heat of mixing ΔE_{inc}^{mix} becomes less sensitive to monomer structure when a single ϵ is chosen for all 66 model blends. The overall range of ΔE_{inc}^{mix} is then only 2.5 (the a–b and l–k model blends give the largest and smallest values).

When a different reference value of $\chi_{eff}^{inc}(\phi_1 = C)$ is available, say from experimental data, eq 3.5 may be used in conjunction with the expressions of Tables I and II to describe $\chi_{eff}^{inc}(\phi_1)$ for arbitrary temperatures T and monomer structures of Figure 1. If the molecular weights are large and the weak dependence on them are neglected, the exchange energy ϵ appropriate to this other case may be obtained approximately from Tables III and IV as follows: Let, for example, the reference value be $\chi_{eff}(\phi_1^{(exp)} = C) = B \neq 0$. The exchange energy parameter ϵ is evaluated (so long as ϵ/k_BT is small) from eq 3.5 as

$$(\epsilon/k_BT) = \frac{B - \chi_S^{(0)}}{\chi_{E_1}^{(0)} + C\chi_{E_1}^{(1)}} \tag{3.7}$$

where the small $\chi_S^{(1)}$, proportional to M_α^{-2}, is neglected. The remaining quantities on the right-hand side of eq 3.7 are either presented in Table II ($\chi_S^{(0)}$) or may be easily determined from the slope $\chi_{eff}^{(1)}$ (in the lower triangle of Table III) and from $(\epsilon/k_BT) \equiv e_{ij}$ (in the upper triangle of Table IV) by

$$\chi_{E_1}^{(1)} = \chi_{eff}^{(1)}/e_{ij} \tag{3.8}$$

$$\chi_{E_1}^{(0)} = -\chi_S^{(0)}/e_{ij} \tag{3.8a}$$

Shifting to other inputs $\chi_{eff}(C)$ by eqs 3.7 and 3.8 still leaves ϵ, ΔE_{inc}^{mix}, and the slope $\chi_{eff}^{(1)}$ as strong functions of monomer structure.

B. Incompressible Model of PS(D)/PVME Blends. This subsection specializes in PS(D)/PVME blends but still retains the incompressibility assumption, as is common in the analysis of small-angle neutron scattering data. Nevertheless, the sensitivity of blend properties to monomer structure is further illustrated by temporarily suspending our knowledge of the styrene and vinyl methyl ether monomer structures and by determining which of the 66 incompressible model binary blends can reproduce the experimental zero-angle neutron scattering data. The smaller the number of successful model blends, the greater the sensitivity of χ_{eff}^{inc} to monomer structures.

Full computations based on Table II show that the 66 model blends yield a slope of χ_{eff}^{inc} vs ϕ_1 that may have either sign and that ranges over 2 orders of magnitude, again exhibiting the strong sensitivity to monomer structure. The microscopic exchange energy (ϵ/k_BT) is chosen for each case separately by fitting to the single-experimental value[6] of χ_{eff} for $\phi_{PSD} = 0.1$ and $T = 142$ °C. The calculations yield four choices having χ_{eff}^{inc} in reasonable agreement with the neutron scattering data of Han et al. These four successful cases correspond, respectively, to the monomer structures k, h, f, and l for styrene and to c, c, c, and b for vinyl methyl ether (VME). The two VME monomer structures b and c are reasonably consistent with the actual monomer structure. Structure b is "exact" if the lattice model invokes an equivalence of CH, O, and CH_3 groups, while structure c has the O–CH_3 occupying a volume equivalent to three C–H subsegment units. The monomer volume ratios $r = \nu_1/\nu_2 = s_1/s_2$ for these four cases are 1.8, 1.4, 1.2, and 2.25, respectively, while the experimental value is $r^{(exp)} = 1.81$. There is more difficulty in accurately representing a benzene ring with flexible bonds on a cubic lattice, but the four styrene monomer structures k, h, f, and l, providing the best fits to the slope $\chi_{eff}^{(1)}$, do crudely capture some essential features of the styrene monomer's shape. Structure l is perhaps the most reasonable shape, given the limitations of a cubic lattice.

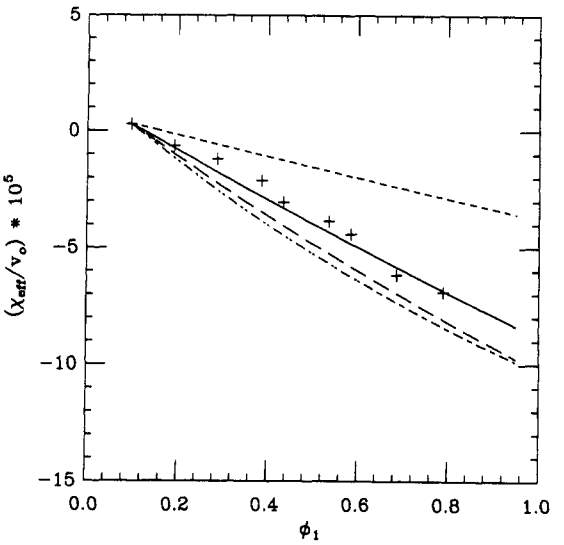

Figure 2. LCT computations of the effective interaction parameter χ_{eff}^{inc} at $T = 142$ °C for four PSD/PVME model incompressible blends. The curves correspond to k–c (– – –), h–c (—), f–c (– –), and l–b (– · · –) model binary blends. The crosses (+) represent the experimental data of Han et al.[6] The molecular weights in computations of Figure 2–4, 6, and 9 are those appropriate to experiments of Han et al.[6] ($M_w^{(PSD)} = 593 \times 10^3$ $M_w^{(PVME)} = 1100 \times 10^3$). The labels of Figures 2–4, 6, and 9 omit the primes, while Figures 2–5 also omit the index *inc*.

The composition dependence of χ_{eff}^{inc} for the four best fit model blends is depicted in Figure 2, where the experimental points (+) of Han et al.[6] for $T = 142$ °C are also included. The LCT calculations for χ_{eff}^{inc} (and χ_{eff}) are presented in Figures 2–4, 6, and 9 as χ'_{eff}/ν_o in order to make a direct comparison with the original experimental data. (Primes, superscripts *inc*, and subscripts *inc*, however, are omitted in the figures.) The h–c blend provides the best fit of the four competing incompressible LCT model blends to the experimental χ'_{eff}/ν_o data at $T = 142$ °C. On the other hand, when the wider temperature range of $T = 100$–142 °C is considered, only the l–b model blend is found to give a reasonably good fit to experiment. However, Figure 3 demonstrates that even this best case exhibits deviations from experiment, especially at the lowest temperature $T = 100$ °C for $\phi_1 = \phi_{PSD} > 0.4$. The quality of the fit to the low-temperature χ_{eff} can more easily be observed in Figure 4, where χ_{eff}^{inc} is presented as a function of $1/T$ for a few compositions of the model incompressible l–b blend. Despite these inaccuracies, the incompressible LCT calculations (with only one adjustable parameter ϵ/k_BT) provide a rather satisfactory description of the neutron scattering data of Han et al.[6] for PSD/PVME blends. The experimental χ'_{eff}/ν_o values are quite small (10^{-5}–10^{-4}), and the fact that the incompressible LCT reproduces them quite accurately over a range of compositions and temperatures and for *realistic* values of the microscopic exchange energy ϵ outweighs the slight discrepancies accentuated in Figure 4.

It is important to check whether the incompressible LCT predictions for excess thermodynamic quantities of

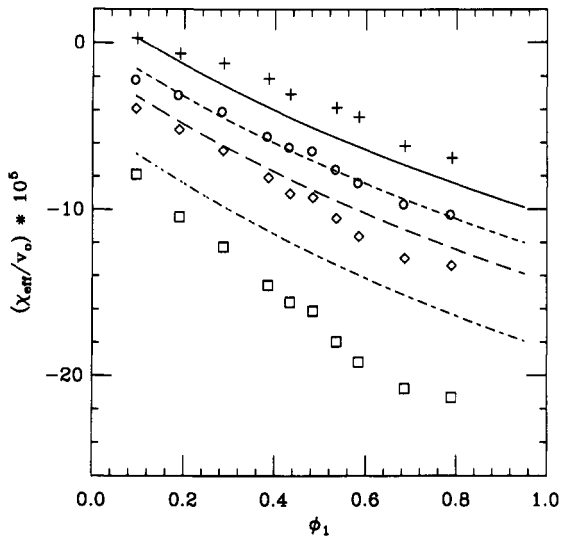

Figure 3. LCT computations of the effective interaction parameters χ_{eff}^{inc} for one of the four PSD/PVME model incompressible blends from Figure 2 (the *l*–*b* blend) at different temperatures. The curves are (—) T = 142 °C, (– – –) T = 130 °C, (– –) T = 120 °C, and (– · · –) T = 100 °C. The experimental points of Han et al.[6] are denoted by crosses (T = 142 °C), circles (T = 130 °C), diamonds (T = 120 °C), and squares (T = 100 °C).

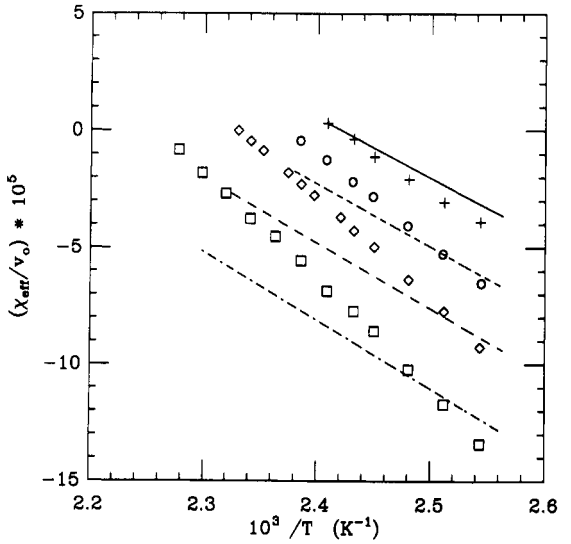

Figure 4. LCT computations for the effective interaction parameter χ_{eff}^{inc} of the *l*–*b* incompressible model for the PSD/PVME blend as a function of $1/T$ for various compositions. The curves from top to bottom correspond to $\phi_1 \equiv \phi_{PSD}$ = 0.1, 0.3, 0.5, and 0.8. Experimental points of Han et al.[6] are represented by crosses (ϕ_1 = 0.1), circles (ϕ_1 = 0.3), diamonds (ϕ_1 = 0.5), and squares (ϕ_1 = 0.8).

PS/PVME blends (like ΔH^{mix}) are likewise consistent with experimental data[7] since no additional adjustable parameters are available for their computations once ϵ is chosen as described above. The incompressible blend LCT heat of mixing, ΔE_{inc}^{mix}, likewise depends on the microscopic exchange energy ϵ and for small ϵ/k_BT becomes roughly proportional to ϵ. The ϵ appropriate to a PS/PVME blend slightly differs from that appropriate to the PSD/PVME system, but, for simplicity, it is assumed that $\epsilon_{PS/PVME} = \epsilon_{PSD/PVME}$. The four examples (that best reproduce the experimental χ_{eff} at T = 142 °C in Figure 2) exhibit very different heats of mixing ΔE_{inc}^{mix} as shown in Figure 5. However, all the ΔE_{inc}^{mix} in Figure 5 are in very poor agreement with experiment; the best case is about a factor of 5 smaller than the experimental data of Shiomi et al.[7] Small differences between $\epsilon_{PS/PVME}$ and $\epsilon_{PSD/PVME}$ are,

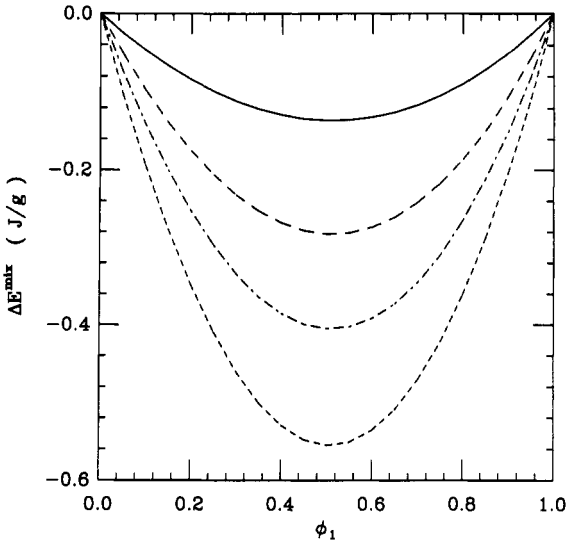

Figure 5. Computed LCT heat of mixing ΔE_{inc}^{mix} at T = 50 °C for the four PSD/PVME model incompressible blends (that best reproduce the experimental χ_{eff} at T = 142 °C from Figure 2). The curves (top to bottom) are for *k*–*c*, *h*–*c*, *f*–*c*, and *l*–*b* model blends. The molecular weights for Figure 5, 7, and 10 are chosen as appropriate to experiments of Shiomi et al.[7] ($M_w^{(PS)}$ = 1.1 × 10^5 and $M_w^{(PVME)}$ = 1 × 10^5). The experimental data of Shiomi et al.[7] are omitted from the figure because they are about a factor of 5 higher than the best theoretical values.

therefore, completely irrelevant here. Another serious deficiency of the incompressible LCT lies in its inability to predict a nonzero volume change on mixing. Experiments[7] for PS/PVME blends at T = 50 °C find $\Delta V^{mix}/(V_1 + V_2)$ of the order of 10^{-3}.

Although the incompressible LCT displays a strong, and therefore interesting, sensitivity of blend properties to monomer structure and although good fits may be obtained to neutron scattering data by using only one input experimental datum, the consideration of the additional properties ΔH^{mix} and ΔV^{mix} leads to rather poor agreement with experiment. The observed nonzero ΔV^{mix} requires the introduction of blend compressibility into the calculations, leaving the questions of whether compressible LCT computations (now with three adjustable parameters ϵ_{11}, ϵ_{22}, and ϵ_{12}) can still reproduce the experimental neutron scattering data with only a small number of the 66 model blends and whether a consideration of other properties, such as ΔH^{mix}, serves to distinguish between the small number of possible fits to the neutron scattering data.

IV. Comparison of the Lattice Cluster Theory Predictions for Scattering and Thermodynamic Properties of PS(D)/PVME Blends with Experimental Data: Role of Compressibility

The compressible blend LCT Helmholtz free energy of mixing ΔF^{mix} is no longer described by a single microscopic exchange energy ϵ. Three independent microscopic energies ϵ_{11}, ϵ_{22}, and ϵ_{12} are required in the simplest possible compressible model. Consequently, the zero-angle neutron scattering parameter χ_{eff} and excess thermodynamic quantities depend for a given temperature T, pressure P, molecular weights $M_w^{(\alpha)}$, and monomer structures on these three different energies $\epsilon_{11} \equiv \epsilon_{S\text{-}S}$, $\epsilon_{22} \equiv \epsilon_{VME\text{-}VME}$, and $\epsilon_{12} \equiv \epsilon_{S\text{-}VME}$. The pressure of P = 1 atm is chosen in all calculations below. The LCT expressions for the compressible χ_{eff} are no longer as analytically simple as χ_{eff}^{inc} in eq 3.5. This occurs, in part, because second-order contributions in $\epsilon_{\alpha\beta}$ as well as contributions of higher order

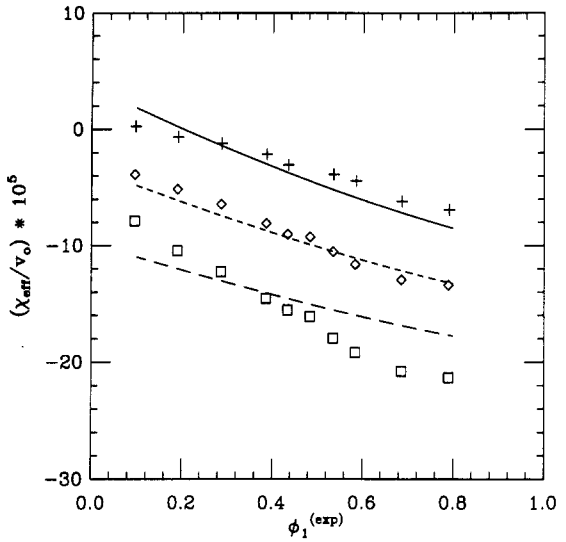

Figure 6. LCT computations of the effective interaction parameter χ_{eff} for the rather unrealistic a–k model for a compressible PSD/PVME blend over the full experimental temperature range. The curves are (—) T = 142 °C, (– – –) T = 120 °C, and (– –) T = 100 °C, while the experimental points of Han et al.[6] are designated with crosses (T = 142 °C), diamonds (T = 120 °C), and squares (T = 100 °C). The three adjustable parameters are found to be ϵ/k_B = 1.245 45 K, ϵ_{11}/k_B = 539.695 K, and ϵ_{22} = 415.15 K.

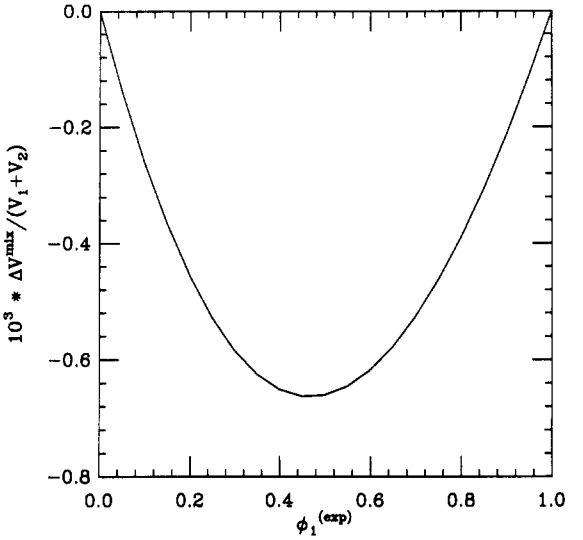

Figure 7. Heat of mixing ΔH^{mix} at T = 50 °C from the LCT unrealistic a–k compressible model for a PS/PVME blend. Same interaction energies as in Figure 6. Data of Shiomi et al.[7] are off scale by roughly a factor of 5.

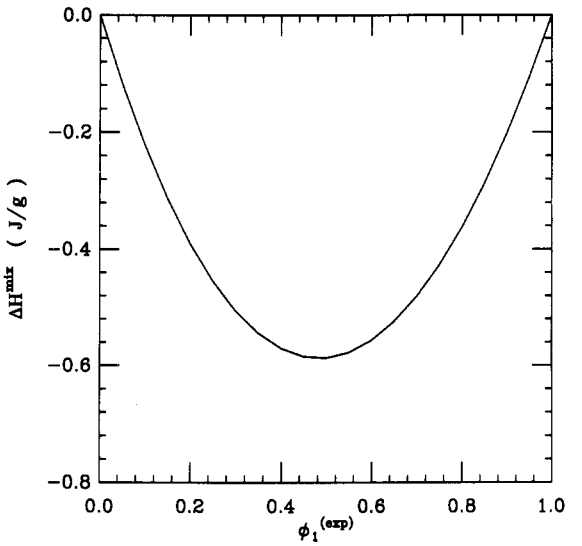

Figure 8. Computed relative volume of mixing $\Delta V^{mix}/(V_1 + V_2)$ at T = 50 °C for the unrealistic a–k compressible model for a PS/PVME blend. Molecular weights are those appropriate to experiments of Shiomi et al.[7] ($M_w^{(PS)}$ = 1.1 × 10⁵ and $M_w^{(PVME)}$ = 5.28 × 10⁴). Energies are the same as in Figure 6.

in compositions become relevant. A rich variety of curves for $\chi_{eff}(\Phi_1)$ are generated in paper 2 from the compressible LCT simply by altering only the self-interaction energies ϵ_{11} and ϵ_{22} at constant ϵ. This feature reflects the algebraic complexity of χ_{eff}, which can be obtained from Table I of paper 2. The three adjustable energy parameters are chosen in the LCT computations below as those providing the best fit to the experimental data of Han et al.[6] over the whole range of temperatures (T = 100–142 °C) and compositions ($\phi_1^{(exp)}$ = 0.1–0.8) for each model blend at the pressure P = 1 atm.

When the compressible LCT is applied only to the SANS data, the presence of three adjustable energy parameters probably leads to more possible fits to the small-angle neutron scattering PSD/PVME data. Because the fitting procedure becomes more tedious than in the incompressible limit, only one such fit is illustrated in Figure 6. The fit to the SANS data[6] in Figure 6 is excellent and is much better than that in Figure 3. However, Figure 6 corresponds to an unrealistic model PSD/PVME blend with monomer structure a for PS and monomer structure k for PVME. The specific volume ratio $r = \nu_S/\nu_{VME}$ = 0.33 for this case differs from the experimental value 1.81 by the most possible from binary blends with the structures in Figure 1. This a–k blend model involves probably the least reasonable structures for this system and is presented here to stress the fact that scattering data alone do not appear to contain enough information to reflect the monomer structures and to determine the three independent interaction parameters of a compressible theory.

Although the rather unrealistic model blend a–k can be made to fit the χ_{eff} data by adjusting the three energy parameters, no additional adjustable parameters are then available for fitting excess thermodynamic properties. Thus, calculations of the heat of mixing ΔH^{mix} and the relative volume of mixing $\Delta V^{mix}/(V_1 + V_2)$ for this a–k model blend provide a more definite test. Figures 7 and 8 display the LCT calculations of ΔH^{mix} and $\Delta V^{mix}/(V_1 + V_2)$, respectively, at T = 50 °C for the a–k model blend. The plots do not include the experimental data because the latter are off scale by roughly a factor of 5 from the theoretical values in Figures 7 and 8. The a–k blend example, thus, emphasizes the need for several independent types of experimental measurements in order to extract meaningful microscopic information. Of course, an adequate theory is also required.

Given the presence of three adjustable energy parameters in the compressible LCT, it is thus sensible to consider all available data for χ_{eff}, ΔH^{mix}, and ΔV^{mix} simultaneously in determining the three energy parameters. We find a reasonably good fit to all these data for only one of the 66 model blends. The successful fit is obtained for a model blend with monomer structure l for PS and b for PVME (a model blend with r = 2.25). The LCT coherent neutron scattering effective interaction parameter $\chi_{eff}(\phi_1^{(exp)})$ for this case in Figure 9 reproduces the SANS experimental data[6] reasonable well over the temperature range T = 100–142 °C) for the choice of parameters ϵ/k_B = 2.9932 K, ϵ_{11}/k_B = 207.575 K, and ϵ_{22}/k_B = 232.484 K. Excess properties are evaluated by using the same energies (no

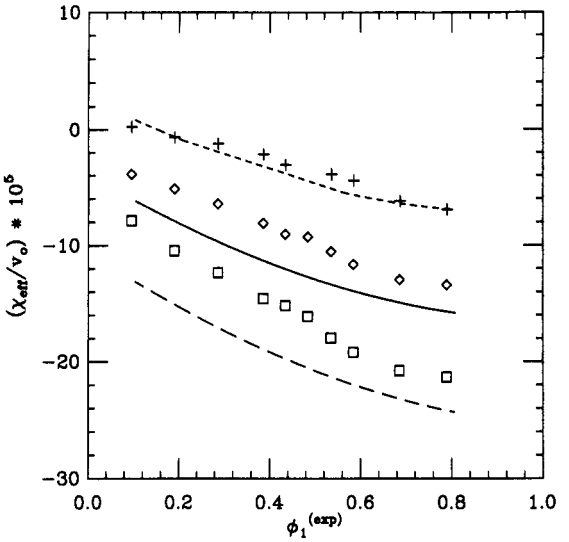

Figure 9. Compressible LCT effective interaction parameter χ_{eff} for the l-b model of a PSD/PVME blend over the full experimental temperature range. The curves correspond to T = 142 °C (- - -), T = 120 °C (—), and T = 100 °C (– –), while the experimental points of Han et al. are specified by crosses (T = 142 °C), diamonds (T = 120 °C), and squares (T = 100 °C). The three adjustable microscopic interaction energies are chosen as ϵ/k_B = 2.933 23 K, ϵ_{11}/k_B = 207.575 K, and ϵ_{22}/k_B = 232.484 K.

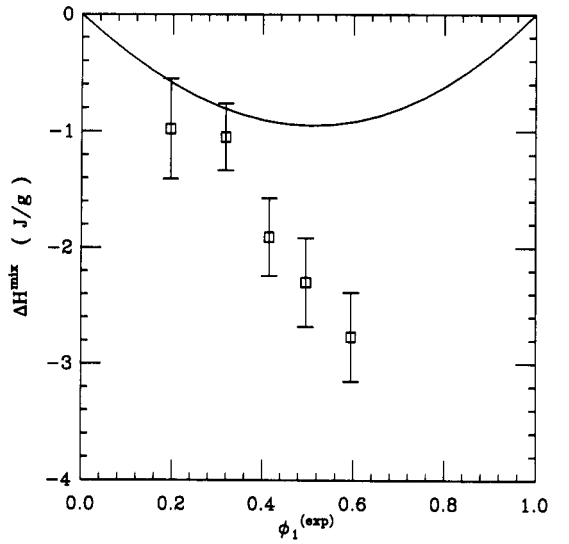

Figure 10. Compressible LCT heat of mixing ΔH^{mix} at T = 50 °C for the l-b model of a PS/PVME blend along with experimental data of Shiomi et al.[7] All energies are the same as in Figure 9.

additional adjustable parameters). Some deviations with experimental data[7] do appear for the heat of mixing ΔH^{mix} and the relative volume of mixing $\Delta V^{mix}/(V_1 + V_2)$ as shown in Figures 10 and 11. The LCT heat of mixing differs from experiment[7] by about 150% for $\phi_1^{(exp)} > 0.4$, while $\Delta V^{mix}/(V_1 + V_2)$ differs from experiment[7] by about 50% for $\phi_1^{(exp)} > 0.4$. A discussion of the origins of the observed discrepancies in Figures 10 and 11 is provided in the next section. Nevertheless, the results in Figures 9–11 again stress the strong sensitivity of macroscopic thermodynamic properties to microscopic monomer structures and interactions and to the compressibilities of real blends as evidenced by their nonzero ΔV^{mix}. The fact that the most realistic l-b model for the PS(D)/PVME blend also provides the best fit to SANS data of Han et al.[6] within the incompressible LCT (see Figure 3) further indicates the importance of monomer molecular structure

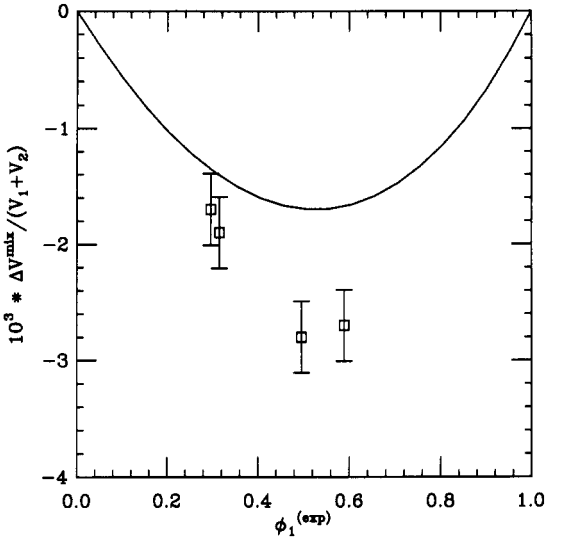

Figure 11. Compressible LCT relative volume of mixing $\Delta V^{mix}/(V_1 + V_2)$ at T = 50 °C for the l-b compressible model of a PS/PVME blend along with data of Shiomi et al.[7] All energies are the same as in Figure 9.

information.

V. Discussion

The lattice cluster theory (LCT) has been used to analyze the influence of monomer molecular structure and compressibility on the thermodynamic properties of binary polymer blends. This analysis consists first in a general depiction of LCT predictions for the variations in blend properties of 66 model binary blends that are composed of vinyl monomers having structures that extend over several lattice sites. Our main interest in this portion of the study lies in the determination of which properties of binary blends are particularly sensitive to monomer structures and to features that are commonly referred to as involving "equation of state effects", i.e., phenomena associated with blend compressibility.[9] The particular blend properties treated are the effective interaction parameter χ_{eff} from extrapolated zero-angle neutron scattering and excess thermodynamic properties. The second part of the analysis involves a comparison of LCT predictions with available small-angle neutron scattering and thermodynamic data for PS(D)/PVME blends. This portion of the study is designed to further the analysis of general trends but also to determine some of the limitations of the extended lattice model upon which the LCT is based.

The lattice cluster theory uses an extension of the standard lattice model of polymers in which each lattice site may house no more than one subunit of either a monomer or solvent molecule. The monomer and solvent molecules are allowed to extend over several lattice sites to more faithfully represent their molecular structures than in the standard lattice model, which assigns all monomers and solvent molecules, no matter what relative size and shape, to lie at single lattice sites. Unoccupied lattice sites are used to model the excess free volume present in any compressible liquid. Because lattice site cells are smaller than monomers or solvent molecules, the description of free volume through unoccupied sites (called voids) by the extended lattice model is somewhat more realistic than in the standard lattice model where voids are the same size as solvent molecules and monomers. However, this generalized lattice model would be for naught if it were approximately treated by classic Flory–Huggins theory[3] because the latter ignores all the corre-

lations that are necessary to distinguish between different monomer structures.

The lattice cluster theory provides systematic corrections to classic FH theory as an expansion in z^{-1}, where the coordination number z is the number of nearest neighbor to a lattice site, and in the microscopic interaction energies $\epsilon_{\alpha\beta}$. An essential feature of the LCT for this study is the fact that a single LCT computation for compressible binary blends provides an analytical expression for the free energy of the blend that is a function of molecular weights, temperature, monomer structures, composition, and microscopic interaction energies. Hence, a wide range of computations may be readily performed for different values of these parameters and for many monomer structures.

Our general study of the influence of monomer structure on blend properties considers 66 model binary vinyl monomer blends. The molecular weights, temperature, and pressure are chosen as appropriate to experiments by Han et al.[6] on PSD/PVME blends, but these choices represent no limitations on the general conclusions. We begin by considering the variability of the neutron scattering χ_{eff} with monomer structure when the incompressibility assumption is applied as is generally done in treatments of neutron scattering data. The 66 model blends exhibit the incompressible χ_{eff} as a linear function of composition ϕ_1. The only adjustable parameter in the incompressible LCT is the exchange energy ϵ, and this is chosen such that χ_{eff} vanishes for $\phi_1 = 0$ in each of the model blends. Different reference values for χ_{eff} or the specification of a common ϵ for all blends leads to similar general conclusions. The slopes of the composition dependence may be of either sign, and for a given sign they are found to vary over several orders of magnitude, thereby displaying an enormous sensitivity of this slope to monomer structure. Likewise, the energies of mixing are found to strongly vary with monomer structures.

When the incompressible LCT is applied to the neutron scattering data of Han et al.,[6] it is found that only four of the model binary blends are reasonably consistent with the experimental data (within factors of roughly 2). This is quite impressive considering that the data are available as a function of both composition and temperature and that there is but one adjustable parameter. The four model blends are found (with no additional adjustable parameters) to yield LCT predictions for the heat of mixing that range over a factor of about 6, but, unfortunately, the best differs from experiment[7] by a factor of 5. The incompressible LCT is also incapable of explaining the considerable volume change in mixing of PS/PVME, so it is natural to study whether compressibility is necessary for a more consistent description of the properties of polymer blends.

The compressible LCT (in its simplest form) has three adjustable parameters, the microscopic interaction energies ϵ_{11}, ϵ_{22}, and ϵ_{12}. We demonstrate that the zero-angle neutron scattering data contain insufficient information to specify these three parameters uniquely by showing that the most unphysical of all possible model blends considered provides an excellent fit to the experimental neutron scattering data. However, requiring that LCT predictions simultaneously reproduce the experimental data for χ_{eff}, ΔH^{mix}, and ΔV^{mix} as functions of composition provides sufficient data to determine these three adjustable parameters. This analysis emphasizes the need for considering several types of experimental data if the desire is to extract meaningful microscopic information from the data concerning the structure and interactions in the blend. It is likewise necessary to employ a theory that is adequate in representing the observed phenomena.

Our lattice cluster theory computations still exhibit deviations from the experimental data, but this is to be anticipated by the fact that the any lattice model represents an oversimplification of reality. Some improvements in describing the experimental data and reality are, in fact, possible within the LCT, but these further extensions lead to additional adjustable parameters. For instance, the LCT computations employ three averaged microscopic interaction parameters. However, it is well-known that, for example, the oxygen in the VME monomer interacts with a different van der Waals energy $\epsilon_{\alpha\beta}$ than do the CH_3, CH_2, or CH groups of that monomer. It is possible to perform LCT computations using such specific interactions, but this would be desirable only if the majority of them are obtained from independent experimental or theoretical data. Likewise, the LCT computations in papers 1 and 2 assume that all junctions are completely flexible, whereas they are in reality semiflexible. It is possible to incorporate semiflexibility[10] into the LCT, but again this can be accomplished at the expense of more adjustable parameters. Therefore, the results of such calculations must undoubtedly improve agreement with experiment. The large number of parameters required in attempts at models of greater reality stresses the importance of using simple models to investigate qualitative variations and general guides for experiments rather than ab initio predictions.

Previous papers in this series[1,2] describe other possible improvements of the lattice model, so it is unnecessary to provide a complete listing. The successes of cell models[11] and equation of state theories[9] suggest the need for using better models of the entropy associated with the distribution of free volume, and this is readily accomplished by replacing the $\phi_\nu \ln \phi_\nu$ in our free energy by more appropriate forms.[9] Likewise, it is straightforward to introduce into the LCT expressions a distance dependence to the ϵ_{ij} as is done by Dee and Walsh,[11] who show how this distance dependence and the free-volume contributions are important features in correctly describing the equations of state for melts under high pressures. Since the applications here are for binary blends at atmospheric pressure, these alterations would be of rather minor consequence. It is the LCT predicted composition dependence of the effective interactions g_{12}, $g_{1\nu}$, and $g_{2\nu}$ in eq 2.2 that exerts a more profound influence on the properties of polymer blends at normal pressures, and these are features that are quite unique in the lattice cluster theory. Equation of state and other phenomenological models introduce composition dependences to these g's in a purely phenomenological fashion through empirical parameters associated with relative surface fractions; however, these surface fractions are not directly related to monomer structures and interactions, nor can they be computed from any molecular type model. The RISM theory of Curro and Schweizer is the only other statistical mechanical theory of polymer blends that proceeds from molecular models.[12] Their integral equation approach uses hard-sphere Lennard-Jones models of monomers, providing a measure of reality (or unreality) that is comparable to that of the lattice cluster theory. Each of these complementary approaches has its relative advantages and disadvantages: A continuum approach is better than a lattice theory,[13] but the lattice model permits the introduction of more intricate and realistic monomer structures, and the final LCT results are produced in an enormously more useable analytic form. It will be interesting to see how RISM

computations fare in comparisons with the PS/PVME data.

Our LCT computations of χ_{eff} assume that the scattering contrast is complete. This is justified because of the very small scattering length of VME. However, there is no difficulty in accounting for incomplete contrast, and this should be done in the general case. Our studies here and in paper 2 demonstrate a strong influence of monomer structure and compressibility on the zero-angle coherent scattering. Thus, it is natural to inquire as to whether structure and compressibility likewise influence the small-angle scattering $S(q)$. Tang and Freed[14] have recently provided the compressible generalization of the random-phase approximation for $S(q)$, and, as will be shown in a subsequent paper, this may be combined with the LCT to investigate the influence of monomer structure on the small-angle scattering.

Paper 4 of this series[15] continues our study of how monomer structure and compressibility affect χ_{eff} by further considering the role of structural asymmetry, temperature, and molecular weights on χ_{eff}. In addition, we evaluate cloud-point curves for several ranges of molecular parameters and monomer structures. The PS/PVME cloud-point curve is computed by using the parameters determined here and is found to be in good agreement with that measured by Han et al.,[6] except near the critical point where fluctuation contributions should be incorporated into the theory, say, from using the compressible RPA.[14] This agreement, however, is to be anticipated because of our reproduction of the SANS data for this system. Of greater interest is our computation for binary compressible blends of closed-loop cloud-point curves and cases with both lower and upper solution critical points.[15] It will be interesting to apply the LCT further in analyzing experimental data on phase diagrams and equations of state for polymer blends.

Acknowledgment. This research is supported, in part, by NSF Grant DMR 89-19941. We are very grateful to Charles Han for assistance in analyzing his SANS experimental data.

References and Notes

(1) Part 1: Dudowicz, J.; Freed, K. F. *Macromolecules*, first of three papers in this issue.
(2) Part 2: Dudowicz, J.; Freed, M. S.; Freed, K. F. *Macromolecules*, preceding paper in this issue.
(3) Flory, P. J. *Principles of Polymer Chemistry*; Cornell University Press: Ithaca, NY, 1953.
(4) Freed, K. F., Bawendi, M. G. *J. Phys. Chem.* **1989**, *93*, 2194 and the references therein.
(5) Dudowicz, J.; Freed, K. F.; Madden, W. G. *Macromolecules* **1990**, *23*, 4803.
(6) Han, C. C.; Baurer, B. J.; Clark, J. C.; Muroga, Y.; Okada, M.; Tran-Cong, Q.; Sanchez, I. C. *Polymer* **1988**, *29*, 2002.
(7) Shiomi, T.; Hamada, F.; Nasako, T.; Yoneda, K.; Nakajima, A. *Macromolecules* **1990**, *23*, 229.
(8) Han, C. C., private communication.
(9) Flory, P. J. *Discuss. Faraday Soc.* **1970**, *49*, 7. Dickman, R.; Hall, C. K. *J. Chem. Phys.* **1986**, *85*, 3023. Honnell, K. G.; Hall, C. K. *J. Chem. Phys.* **1989**, *90*, 1841.
(10) Bawendi, M. G.; Freed, K. F. *J. Chem. Phys.* **1987**, *86*, 3720.
(11) Dee, G. T.; Walsh, D. J. *Macromolecules* **1988**, *21*, 811, 815.
(12) Schweizer, K. S.; Curro, J. G. *J. Chem. Phys.* **1989**, *91*, 5059.
(13) Freed, K. F. *J. Chem. Phys.* **1989**, *90*, 3261.
(14) Tang, H.; Freed, K. F. *Macromolecules* **1991**, *24*, 958.
(15) Freed, K. F.; Dudowicz, J., *Theor. Chim. Acta*, in press.

Registry No. PS (homopolymer), 9003-53-6; PVME (homopolymer), 9003-09-2.